Ion mass estimations by the Swarm electric field instrument (EFI)

Matthias Förster[1], Johnathan Burchill[2], and Levan Lomidze[2]
(mfo@gfz-potsdam.de)

(1) - GFZ German Research Centre for Geosciences, Section 1.1, 14473 Potsdam, Germany
(2) - Department of Physics and Astronomy, University of Calgary, Calgary, Alberta, Canada

Swarm 10th anniversary & science conference 2024
April 08–12, 2024, Copenhagen, Denmark

Electric Field Instrument (EFI)
poster 62

Abstract

The present default Langmuir Probe (LP) algorithm for estimating the plasma density relies on three major suppositions: the orbital motion limited (OML) theory is applicable, the surrounding plasma consists of pure oxygen ions only, and the along-track ion velocity coincides with the spacecraft orbital speed. These assumptions are routinely violated, particularly with respect to ion composition on the nightside and during periods of low solar activity as well as at auroral and polar latitudes, where ion drifts of magnetospheric origin are dominating. Both factors are compromising the accuracy of the plasma density measurements. Further, numerical simulations of the spacecraft's plasma environment and observational results have shown that plasma shielding effects are not negligible. These effects have been taken into account with the novel SLIDEM (Swarm LP Ion Drift and Effective Mass) product, which also yields improved estimates of the plasma density, the along-track ion drift and the effective ion mass along the orbital path. This is done by additional use of the ion current to the faceplate at Swarm's front side. It will be shown, that the measurements of the Langmuir probe alone can result in reliable ion mass and accordingly revised plasma density estimations.

Langmuir probes as part of the Electric Field Instrument (EFI)

Fig. 1. The figure shows the front view of the Swarm satellites with the Thermal Ion Imager (TII) and its vertical and horizontal sensors mounted on a rectangular plate ("frontplate", FP) in the center and the two spherical Langmuir Probes at the bottomside. The front plate of the CEFI instrument allows with a fixed negative bias (-3.5 V) the estimation of the ram plasma density with 16 Hz resolution during periods, when the Thermal Ion Imager (TII) is off.

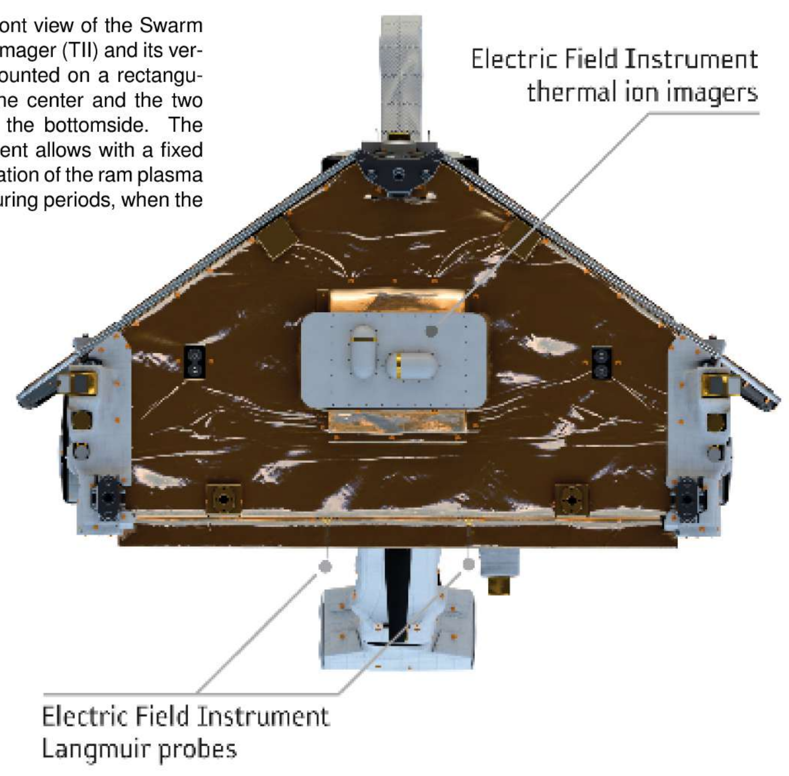

The two spherical Langmuir probes, which are coated with nitrated titanium (TiN) and gold-plated titanium (Au), respectively, are working with different sensitivities, called "low and high gain", to cover the large dynamic range in the F-layer ionosphere, which is probed by Swarm (Buchert and Nilsson, 2016; Knudsen et al., 2017). Electron temperature (T_e) and plasma potential (f_p) values are estimated by applying a sinusoidally varying bias in the linear electron current region of the U-I characteristics, the position of which is at a fixed offset from the tracked bias potential (zero current). The electron density (N_e) is always derived from the real admittance (the derivative) in the ion current region.

For a negatively biased (usually -3.5 V) EFI faceplate, taken as a planar probe with an area of 804 cm^2 (Knudsen et al., 2017) ignoring edge effects and assuming quasi-neutrality ($N_e = N_i$), the ion current I_{FP} amounts to:

$$I_{FP} \quad = \quad -N_e \; e \; u_{i,ram} \; A_{FP} \tag{1}$$

where the total ion number density N_i, the electric charge unit e, the ion flow speed $u_{i,ram}$, and the faceplate area A_{FP} are expressed in conventional units. The theoretical basis for the spherical LP current measurements is the "orbital motion limited (OML)" approach according to Mott-Smith and Langmuir (1926). At sufficiently negative bias (usually -2.5 V) and neglecting the photoelectrons the current is (equ.(1) in Buchert and Nilsson (2016)):

$$I_{ion} \quad = \quad \begin{cases} -\pi r_p^2 \; e \; u_i \; N_e[1-\frac{(V_b+V_S)}{E_i}] & , \quad V_b+V_S < E_i \\ 0 & , \quad V_b+V_S \geq E_i \end{cases} \tag{2}$$

with r_p as probe radius, V_b its bias voltage (-2.5 V), V_S the satellite potential, and E_i the ion ram energy, which is supposed to be the S/C velocity ($\sim 7.6 \; km/s$) in the first approximation. E_i is given in units of electron volt (eV) as $E_i = m_i \; u_i^2/(2e)$. The Swarm LP ion densities that result from equation (2) were originally derived for a single-species (O^+) ionosphere (Buchert and Nilsson, 2016). The analysis within the SLIDEM project (Pakhotin et al., 2022), however, has been generalized to multiple ion species with the effective ion mass M_{eff} defined as:

$$\frac{1}{M_{eff}} \quad = \quad \frac{1}{N_i}\sum_{k=1}^{n} N_{i,k}\frac{1}{m_{i,k}} \qquad \text{where} \quad N_i = \sum_{k=1}^{n} N_{i,k} \tag{3}$$

One full solar activity cycle of measurements

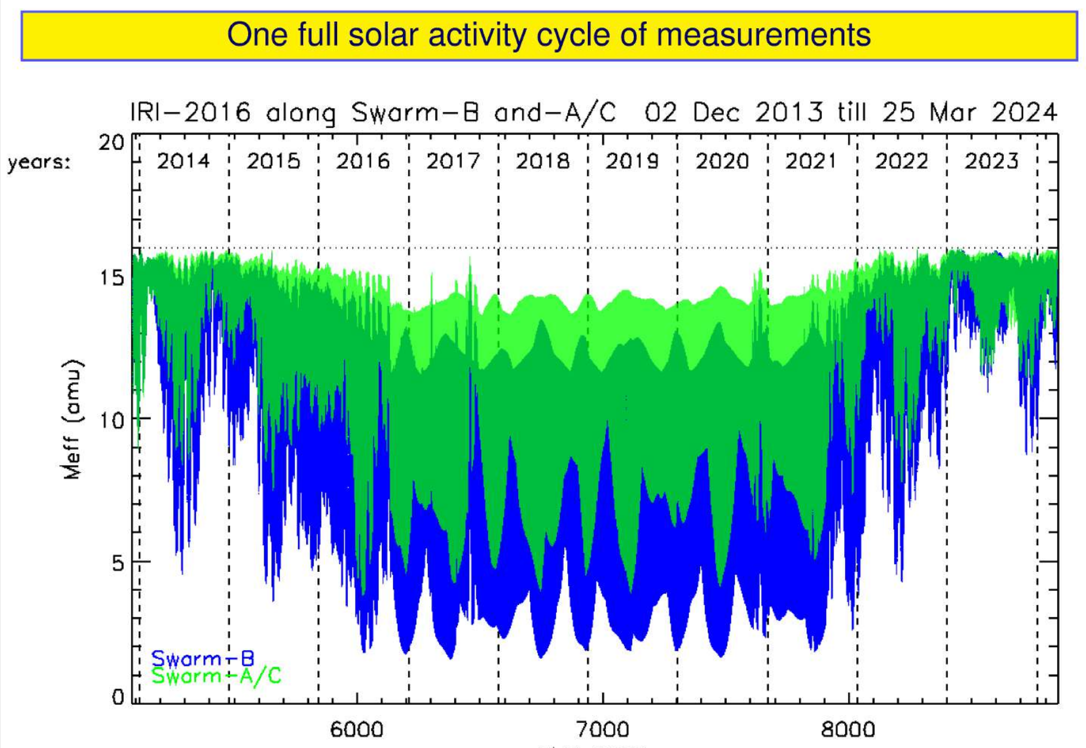

Fig. 2. Predictions of effective ion masses M_{eff} along the Swarm satellite orbits according to the empirical model of the International Reference Ionosphere 2016 (IRI-2016) for the whole measurement interval of the Swarm mission up to now (Dec 2013 – March 2024). It comprises approximately one full solar cycle of solar activity. The minimum-maximum ranges of M_{eff} along full circular, polar orbits are shown for each orbit of the Swarm-A and -C satellites (in green color) as well as for the higher up orbiting Swarm-B (in blue, partly "below" the green ones). Long-term and short-term solar activity dependences (cf. Fig. 3) are clearly visible.

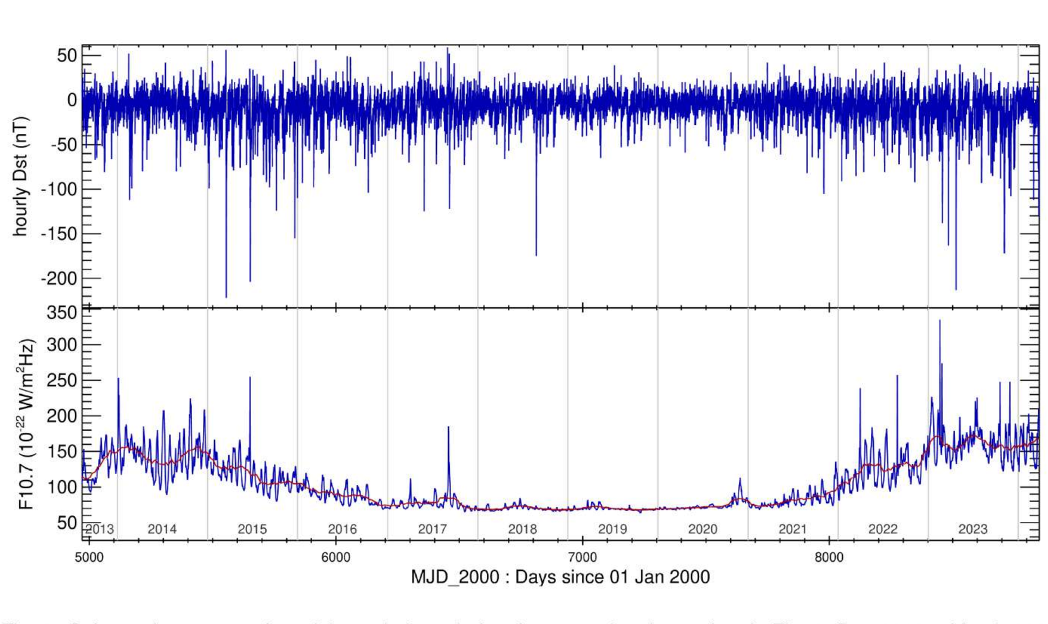

Fig. 3. Solar and geomagnetic activity variations during the same time interval as in Fig. 2, Dec 2013 – March 2024, according to the parameters: 1.) Geomagnetic Equatorial Disturbance storm time index (Dst, upper panel) in units of [nT] and 2.) the Solar Radio Flux at 10.7 cm wavelength (2800 MHz), known as F10.7 index (bottom panel) in s.f.u. of [10^{-22} W m^{-2} Hz^{-1}]. The abszissa shows the time progression in Modified Julian Days since Jan 1st, 2000 (MJD_2000). The individual yearly periods are indicated by numbers at the bottom of the plot.

Langmuir probe: theoretical basis and model approach

The first derivative (or admittance) d_{ion} results from equ. (2) to (Pakhotin et al., 2022):

$$d_{ion} \quad = \quad \partial I/\partial V_b \quad = \quad 2\pi r_p^2 \, e^2 \, N_e/(M_{eff} \; u_i) \tag{4}$$

According to the SLIDEM methodology, the ion admittance and faceplate currents are used to estimate of ion density and the along-track ion drift by solving equations (1) and (4) simultaneously rather than independently, yielding also the effective ion mass M_{eff} this way (see also: Burchill and Lomidze, 2024):

$$N_e = \sqrt{\frac{d_i I_{FP} M_{eff}}{2e^3 A_{FP} \pi r_p^2}} \qquad v_i = \sqrt{\frac{2e\pi r_p^2 I_{FP}}{d_i A_{FP} M_{eff}}} \qquad M_{eff} = \frac{2e^2 \pi r_p^2 N_e}{d_i v_i} \tag{5}$$

The OML theory is valid, if the probe radius r_p is small compared with the sheath's thickness that surrounds it, and the LP itself should be mounted outside of the satellite's sheath, which can be estimated by the Debye shielding distance. According to Brace (1998) a boom length of 30 to 100 cm is adequate for most ionosphere applications. In a magnetized plasma, which is probed by the Swarm satellites at LEO, the electron dynamics are controlled by the strenght and direction of the geomagnetic field (Marchand, 2016; Miyake et al., 2020; Resendiz Lira and Marchand, 2021).

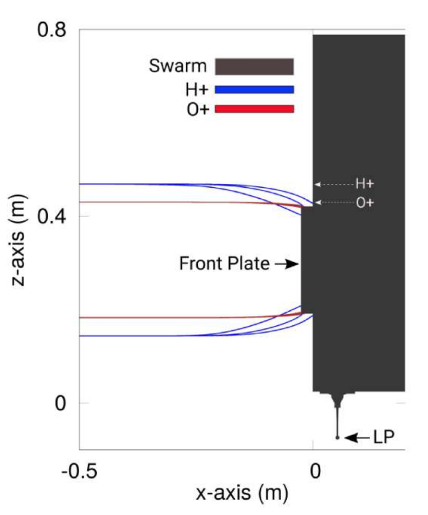

Fig. 4. Ion trajectories of O^+ (red) and H^+ (blue) are deflected near the FP due to curved equipotentials near the satellite and FP's perimeter. Both species are aimed slightly below or above (dashed arrows) the FP with velocities exactly from the ram direction. Three speeds are considered: the ram speed (equal to v_{sat}), and the ram speed $\pm v_{th}$, the ion's thermal speed with $v_{th} = \sqrt{\frac{2kT}{m}}$ (from Resendiz Lira et al., 2019, Fig. 6).

A series of numerical simulations with various parameters resulted in an approximative correction formula as:

$$I_{FP} = -N_e \; e \; u_{i,ram} \; A_{geo}(1+\delta_{model}) \tag{6}$$

With:

$$\delta_{\text{model}} = \frac{\alpha P \lambda_D}{A_{\text{geo}}}\left(1 - \frac{eV}{\frac{1}{2}m_{\text{eff}}v_\perp^2} - \beta\frac{eV}{kT_e} - \frac{\gamma}{eV}\frac{e^2}{4\pi\epsilon_0\lambda_D}\right)$$

Where P is the perimeter of the FP (the sum of the length of all sides), V is the plate potential with respect to background plasma, T_e is the electron temperature, and λ_D the electron Debye length. α, β, and γ are fitting parameters. Their optimal values were found by (Resendiz Lira et al., 2019) to be 0.06929, 0.11552, and 66.0913 x 10^6, respectively.

A similar empirical correction was found by a series of three-dimensional kinetic simulations using the PTetra model (Marchand, 2012) and applying a large bundle of typical ionospheric conditions to obtain an optimal correction term (Resendiz Lira and Marchand, 2021, equ. 14) for the LP ion current:

$$I_{ion} \quad = \quad -\pi r_p^2 \; e \; u_i \; N_e[1-\frac{(V_b+V_S)}{E_i}](1-\delta) \tag{7}$$

With (Resendiz Lira and Marchand, 2021, equ. 15):

$$\delta = \alpha\frac{\lambda_D}{r_p}\left(1 - \beta\frac{eV_f}{\frac{1}{2}m_{eff}v_d^2} - \gamma\frac{eV_f}{kT_e}\right) - \zeta V_f + \xi. \tag{15}$$

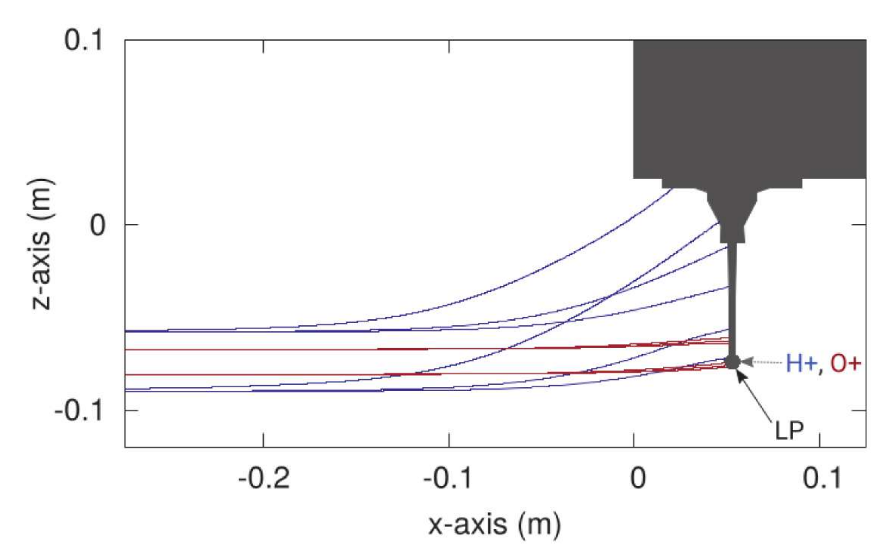

Fig. 5. O^+ (red) and H^+ (blue) ion trajectories deflected in the satellite sheath when the spherical probes are operated in the ion saturation region. Both species are aimed slightly below or above the spherical probe with velocities exactly from the ram direction. Particles with lower energy (speed and mass) are deflected the most, and the ones with the higher speed and mass are deflected the least.

The M_{eff} values in this study are derived from the high-gain Swarm Langmuir probe alone using equations 4 and 7 above, i.e., as ratio of the ion current and its admittance in the ion acceleration regime. This has the advantage, that the direct dependence on plasma density cancels out, the along-track ion drift motion, however, that is governed by $\boldsymbol{V} = \boldsymbol{E}\times\boldsymbol{B}/|B|^2$ dominates at high latitudes (mlat $\geq \sim \pm 50°$) and can be calculated there independently (and the like the re-estimated plasma density).

Estimations of the effective ion mass

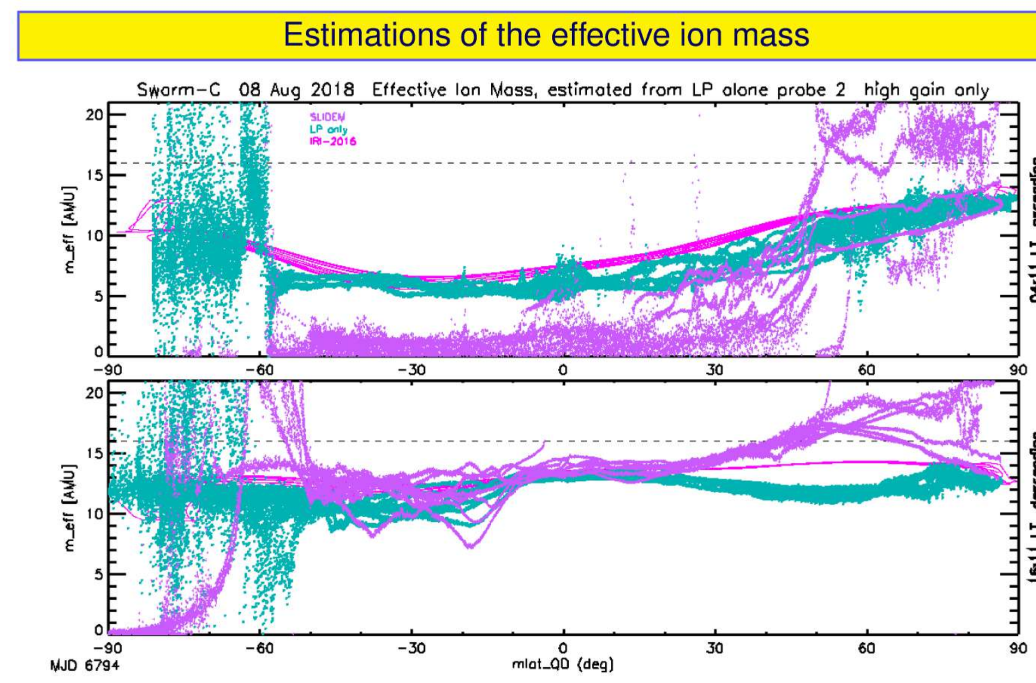

Fig. 6. Comparison of estimated effective ion masses M_{eff} for Swarm-C on Aug 08, 2018, as obtained from SLIDEM (violet curves), resulting from LP measurements as ratio of ion current and ion admittance (teal curves), and according to the IRI-2016 empirical model, calculated along the satellite orbit (magenta). The M_{eff} records are shown versus magnetic QD-latitude for ascending (upper panel) and descending (bottom panel) orbital parts.

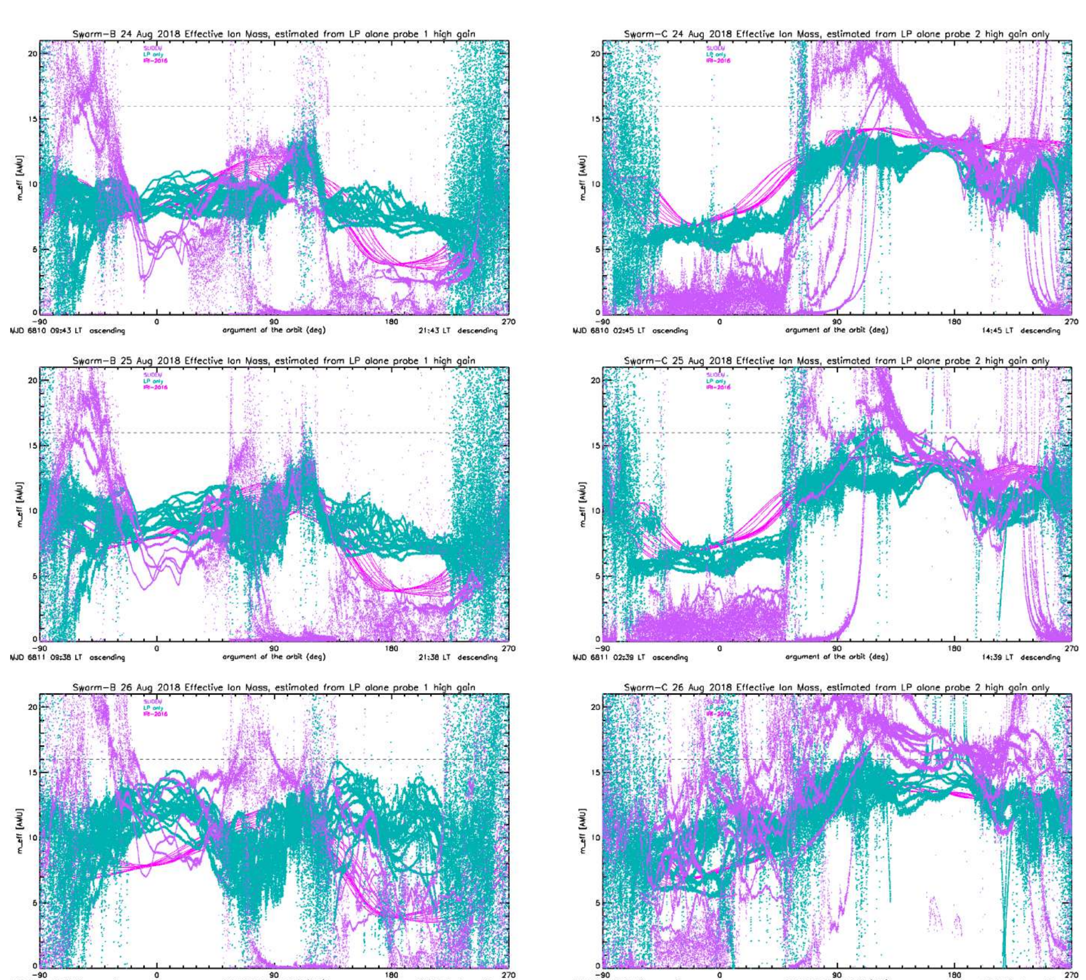

Fig. 7. Estimated effective ion mass values M_{eff} like in Fig. 6 above, but drawn here for full orbits of the three days Aug 24-26, 2018, versus argument of orbit. The left column shows Swarm-B observations along a prenoon-premidnight orbit (~10–22 LT), while the right column shows Swarm-C measurements along an early morning-afternoon orbit (~03–15 LT). The left half of each panel exhibits ascending orbital parts, while the right half displays the descending parts. The three days cover a geomagnetic storm interval with minimum-Dst values of -175 nT on 05 UT on Aug 26, 2018, and Kp values up to 7+. Enhanced M_{eff} values are clearly visible on the last (storm) day of the interval. The dashed horizontal lines indicate pure oxygen ion dominance (M_{eff} = 16).

Long-term variation of the effective ion mass M_{eff}

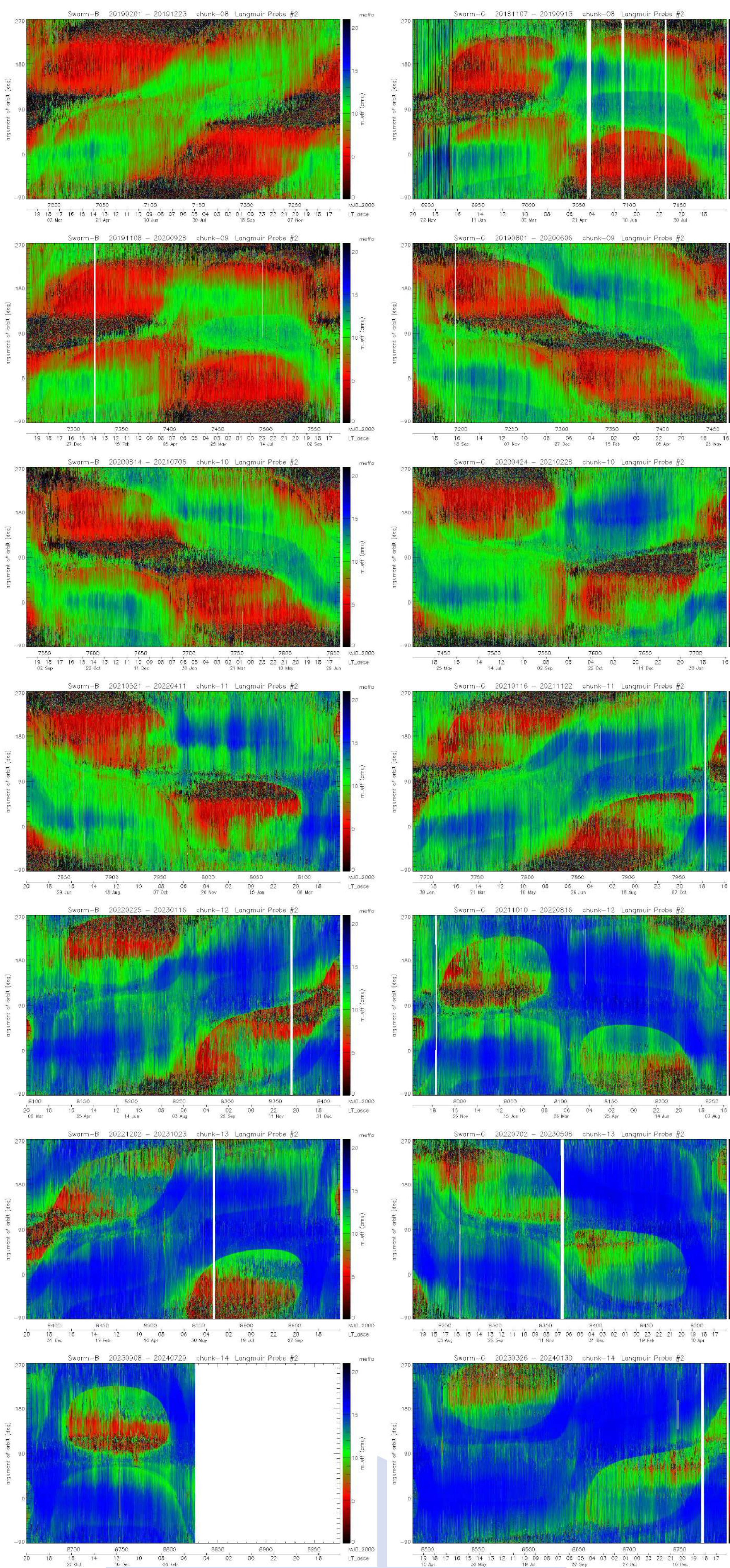

Fig. 8. Long-term variation of M_{eff} , as estimated from the ion current and admittance of the high-gain Langmuir probe alone using equations 7 and 4, respectively. The latest seven full chunk intervals (Nos. 8 through 14) for about the last five years are shown that cover each all local times for both ascending and descendig orbital branches. The ordinate is drawn along the orbital path as so-called argument of orbit with equatorial crossings at 0°and 180°for the ascending and descending branches, respectively. Valid M_{eff} estimations are confinded to ±50°around the equtorial crossings, while the auroral and polar regions are affected by large along-track drift.

Storm-time variation of the effective ion mass M_{eff}

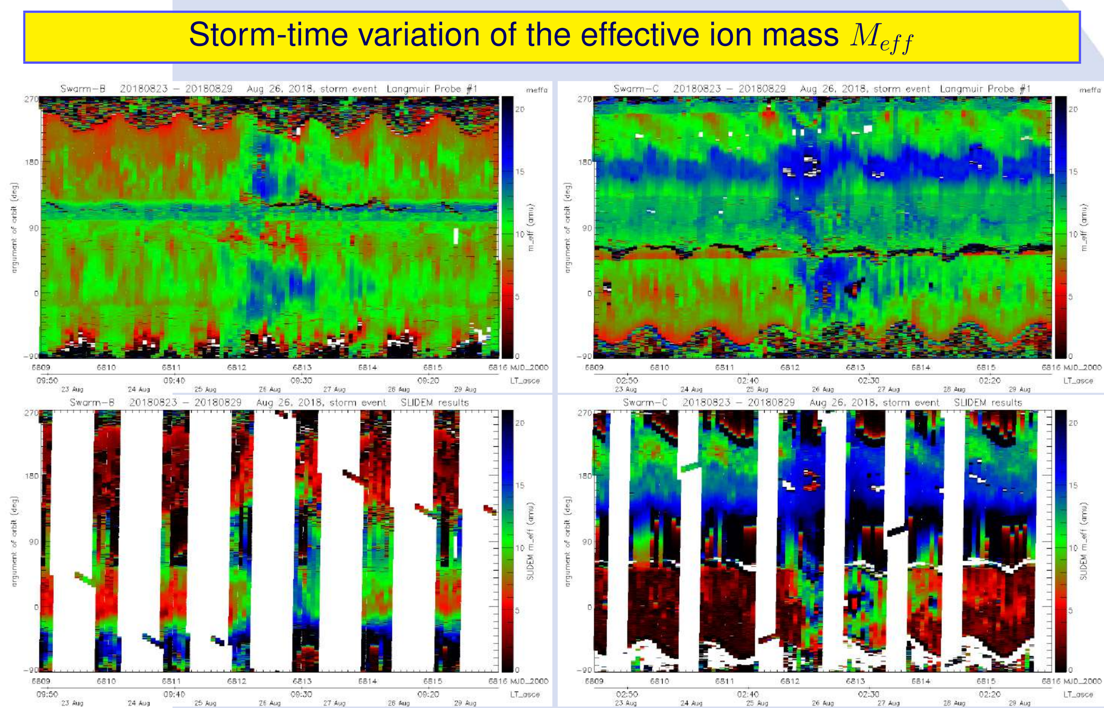

Fig. 9. Zoomed-in variation of effective ion mass M_{eff} during a few days around the geomagnetic storm event of August 26, 2018 (cf. middle column, bottom) for both Swarm-B (left side) and Swarm-C (right) records. The upper panels show M_{eff} as estimated from the ion current and admittance of the high-gain Langmuir probe alone as plotted in Fig. 8 for full-chunk intervals. The bottom panels show the same satellite records during the same storm period, but with the results from the SLIDEM data set. The storm event is clearly marked by a pronounced increase of M_{eff} and the subsequent gradual return to prestorm conditions with minor differences due to the actual local time during Swarm overflights.

References

Brace, L. H.: Langmuir probe measurements in the ionosphere, vol. 102 of *Geophysical Monograph*, pp. 23–35, American Geophysical Union, 1998.

Buchert, S. and Nilsson, T.: Langmuir Probe Level 1b Algorithm, Swedish Institute of Space Physics (IRFU), Sweden, SW-TN-IRF-EF-003, Rev.: 3, 2016-12-01 edn., 2016.

Burchill, J. K. and Lomidze, L.: Calibration of Swarm ion density, drift, and effective mass measurements, Earth and Space Science, 11, e2023EA003463, doi:10.1029/2023EA003463, 2024.

Knudsen, D. J., Burchill, J. K., Buchert, S. C., Eriksson, A., Gill, R., Wahlund, J.-E., Ahlen, L., Smith, M., and Moffat, B.: Thermal Ion Imagers and Langmuir Probes in the Swarm Electric Field Instruments, J. Geophys. Res., 122, 2655–2673, doi:10.1002/2016JA022571, 2017.

Marchand, R.: PTetra, a Tool to Simulate Low Orbit Satellite–Plasma Interaction, IEEE Trans. Plasma Sci., 40, 217–229, doi:10.1109/TPS.2011.2172638, 2012.

Marchand, R.: Ionospheric Langmuir probe electron temperature asymmetry and magnetic connectivity, IEEE Transactions on Plasma Science, 99, 1923–1926, doi:10.1109/TPS.2016.2619668, 2016.

Miyake, Y., Miloch, W. J., Kjus, S. H., and Pécseli, H. L.: Electron Wing-Like Structures Formed at a Negatively Charged Spacecraft Moving in a Magnetized Plasma, J. Geophys. Res., 125, doi:10.1029/2019JA027379, 2020.

Mott-Smith, H. M. and Langmuir, I.: The theory of collectors in gaseous discharges, Phys. Rev., 28, 727–763, 1926.

Pakhotin, I. P., Burchill, J. K., Förster, M., and Lomidze, L.: The Swarm Langmuir Probe Ion Drift, Density and Effective Mass (SLIDEM) Product, Earth, Planets and Space, 74:109, doi:10.1186/s40623-022-01668-5, 2022.

Resendiz Lira, P. A. and Marchand, R.: Simulation Inference of Plasma Parameters From Langmuir Probe Measurements, Earth and Space Science, 8, –, doi:10.1029/2020EA001344, 2021.

Resendiz Lira, P. A., Marchand, R., Burchill, J., and Förster, M.: Determination of Swarm front plate's effective cross section from kinetic simulations, IEEE Trans. Plasma Sci., 47, 3667–3672, doi:10.1109/TPS.2019.2915216, 2019.